CONSERVATION OF MOIST POTENTIAL VORTICITY AND DOWN-SLIDING SLANTWISE VORTICITY DEVELOPMENT*

Wu Guoxiong (吴国雄), *Cai Yaping* (蔡雅萍) and *Tang Xiaojing* (唐晓菁)

State Key Laboratory of Numerical Modeling for Atmospheric Sciences and Geophysical Fluid Dynamics (LASG), Institute of Atmospheric Physics, Chinese Academy of Sciences, Beijing 100080

Received January 11, 1996

ABSTRACT

An accurate form of the moist potential vorticity (MPV) equation was deduced from a complete set of primitive equations. It was shown that motion in a saturated atmosphere without diabatic heating and friction conserves moist potential vorticity. This property was then used to investigate the development of vertical vorticity in moist baroclinic processes. Results show that in the framework of moist isentropic coordinate, vorticity development can result from reduction of convective stability, or convergence, or latent heat release at isentropic surfaces. However, the application of the usual analysis of moist isentropic potential vorticity is limited due to the declination of moist isentropic surfaces, and a theory of development based on z-coordinate and p-coordinate was then proposed. According to this theory, whether the atmosphere is moist-symmetrically stable or unstable, or convective stable or unstable, the reduction of convective stability, the increase of the vertical shear of horizontal wind or moist baroclinity may result in the increase of vertical vorticity, so long as the moist isentropic surface is slantwise. The larger the declination of the moist isentropic surface, the more vigorous the development of vertical vorticity. In a region with a monsoon front to the north and the warm and moist air to the south, or by the north of the front, the moist isentropes are very steep. The is the region most favorable for development of vorticities and formation of torrential rain.

For a case of persistent torrential rain occurring in the middle and lower reaches of the Changjiang and Huaihe Rivers in June 11−15, 1991, moist potential vorticity analysis, especially the isobaric analysis of its vertical and horizontal components, i. e. MPV1 and MPV2, respectively, is effective for identifying synoptic systems not only in middle and high latitudes, but also in low latitudes and in the lower troposphere. It can serve as a powerful tool for the diagnosis and prediction of torrential rain.

Key words: moist potential vorticity (MPV), slantwise vorticity development (SVD), moist-symmetrical instability

I. INTRODUCTION

The occurrence and development of torrential rain are usually associated with the rapid developments of convergence of low-layer flow and rising motion, accompanied by dramatic growth of vertical cyclonic vorticity. The mechanism of development of cyclonic vorticity is therefore one of the important issues in the study of torrential rain occurrence (Tao 1980). Some scientists use linearized perturbation equation and eigenmode analysis techniques to study

* This study was supported by the Key Program No. 49635170 and Program No. 49575265 of the National Natural Science Foundation of China.

the variations of each eigenmode under different background fields. Others, by virtue of conservation of some atmospheric properties, say energy, study the development of one particular scale system through the transition of such properties from other scale systems. Among these, there exists an accurate conservation property, i. e. the Ertel potential vorticity (Ertel 1942)

$$P_E = \alpha \boldsymbol{\zeta}_a \cdot \nabla \theta,$$

provided the atmospheric motion is adiabatic and frictionless. Here α is specific volume, θ is potential temperature, and $\boldsymbol{\zeta}_a$, the 3-dimensional absolute vorticity vector. The application of Ertel potential vorticity in the diagnosis of atmospheric motion has been summarized by Hoskins et al. (1985). Generally speaking, P_E is indicative of some aspects of the movement and development of weather systems in middle and high latitudes. However, in the lower troposphere, especially at low latitudes, P_E becomes very weak. Besides, P_E does not include the effects of moisture. Thus the application of P_E analysis is not so good in the lower troposphere, low latitude regions and in precipitation cases.

Based on the Boussinesq approximation, Bennetts and Hoskins (1979) considered the impact of moisture. The purposes of this study are, by using primitive equations, to introduce the effects of latent heat release due to moisture condensation into the analysis of potential vorticity, so as to study the development of the vertical component of vorticity associated with the occurrence of torrential rain. In Section II, an equation of variation of moist potential vorticity (MPV) is deduced from the primitive equation set. Conservation of MPV in a saturated atmosphere under adiabatic and frictionless conditions is proved in Section III. Based on this conservation property, the characteristic of MPV and the associated theory of vorticity development in the frameworks of moist isentropic, geometric and isobaric coordinate are investigated in Sections IV, V and VI. It is also shown how the increases in the vertical shear of horizontal wind and moist baroclinity can result in the vigorous development of vertical cyclonic vorticity, provided the moist isentropic surface is slanting. In Section VII, the application of the theory to the analysis and prediction of torrential rain is examined by diagnosing the occurrence and evolution of a persistent torrential rainfall process occurring in the middle and lower reaches of Changjiang and Huaihe Rivers in June 11—15, 1991. Some discussions and conclusions are given in Section VIII.

II. EQUATION OF MOIST POTENTIAL VORTICITY

Taking the vector-curl of the primitive momentum equation

$$\frac{\partial \boldsymbol{V}}{\partial t} + \nabla\left(\frac{V^2}{2} + \varphi\right) - \boldsymbol{V} \times \boldsymbol{\zeta}_a = - \alpha \nabla P + \boldsymbol{F}_v, \tag{1}$$

one obtains the following vorticity equation

$$\frac{\partial \boldsymbol{\zeta}_a}{\partial t} - \nabla \times (\boldsymbol{V} \times \boldsymbol{\zeta}_a) = \nabla P \times \nabla \alpha + \boldsymbol{F}_\zeta, \tag{2}$$

where $\boldsymbol{V}$ is 3-D wind vector, $\boldsymbol{\zeta}_a$ absolute vorticity, φ potential function for external forcing; $\boldsymbol{F}_v$ surface friction; and $\boldsymbol{F}_\zeta = \nabla \times \boldsymbol{F}_v$, vorticity generation due to surface friction. Let $\boldsymbol{\Omega}$ denote the angular velocity of the earth, then

$$\boldsymbol{\zeta}_a = \nabla \times \boldsymbol{V} + 2\boldsymbol{\Omega}. \tag{3}$$

The thermodynamic equation including latent heat release and other kinds of diabatic heating Q_d can be written as

$$C_p \frac{T}{\theta}\frac{D\theta}{Dt} = -L\frac{Dq}{Dt} + Q_d, \tag{4}$$

in which all quantities are conventional, and $\frac{D}{Dt} = \frac{\partial}{\partial t} + \boldsymbol{V}\cdot\nabla$. Introducing the following definition of equivalent potential temperature

$$\theta_e = \theta\exp\left(\frac{L}{c_p}\frac{q}{T}\right) \tag{5}$$

into (4) results in a new form of thermodynamic equation

$$\frac{D\theta_e}{Dt} = \left(\frac{\partial}{\partial t} + \boldsymbol{V}\cdot\nabla\right)\theta_e = \frac{\theta_e}{c_p T}Q_d \equiv Q. \tag{6}$$

Taking a scalar product between (2) and $\nabla\theta_e$, and using the following identities

$$\nabla\theta_e\cdot\nabla\times(\boldsymbol{V}\times\boldsymbol{\zeta}_a) = -\nabla\cdot[\nabla\theta_e\times(\boldsymbol{V}\times\boldsymbol{\zeta}_a)],$$

$$\nabla\theta_e\times(\boldsymbol{V}\times\boldsymbol{\zeta}_a) = \boldsymbol{V}(\boldsymbol{\zeta}_a\cdot\nabla\theta_e) + \boldsymbol{\zeta}_a\left(\frac{\partial\theta_e}{\partial t} - Q\right),$$

give

$$\left(\frac{\partial}{\partial t} + \boldsymbol{V}\cdot\nabla\right)(\boldsymbol{\zeta}_a\cdot\nabla\theta_e) + (\boldsymbol{\zeta}_a\cdot\nabla\theta_e)\nabla\cdot\boldsymbol{V}$$
$$= (\nabla P\times\nabla\alpha)\cdot\nabla\theta_e + \nabla\theta_e\cdot\boldsymbol{F}_\zeta + \boldsymbol{\zeta}_a\cdot\nabla Q. \tag{7}$$

Upon multiplying the above equation by specific volume α and by virtue of the equation of continuity of mass

$$\frac{D\alpha}{Dt} - \alpha\nabla\cdot\boldsymbol{V} = 0. \tag{8}$$

the following equation can be reached

$$\frac{DP_m}{Dt} = \alpha(\nabla P\times\nabla\alpha)\cdot\nabla\theta_e + \alpha\nabla\theta_e\cdot\boldsymbol{F}_\zeta + \alpha\boldsymbol{\zeta}_a\cdot\nabla Q, \tag{9}$$

where

$$P_m = \alpha\boldsymbol{\zeta}_a\cdot\nabla\theta_e \tag{10}$$

is the potential vorticity for a moist saturated atmosphere, or simply, moist potential vorticity (MPV). It is equal to the product between $|\nabla\theta_e|$ and the projection on $\nabla\theta_e$ of the absolute vorticity of the air. Equation (9) is the accurate form of MPV equation.

III. CONSERVATION OF MOIST POTENTIAL VORTICITY

A frictionless and moist adiabatic atmosphere satisfies

$$\boldsymbol{F}_\zeta = 0, \qquad Q = 0,$$

and the MPV equation (9) now becomes

$$\frac{DP_m}{Dt} = \alpha(\nabla P\times\nabla\alpha)\cdot\nabla\theta_e, \qquad (\boldsymbol{F}_\zeta = 0,\ Q = 0). \tag{11}$$

Notice that the area integral of the solenoid term $(\nabla P\times\nabla\alpha)$ over an unit cross-section equal to the work done by pressure gradient force along its border curve, and that, according to Eq. (2), the amount of the work equals the amount of change in absolute vorticity over the cross-section. Thus, the physical meaning of (11) is readily understood: the material change of MPV equals the product between $|\nabla\theta_e|$ and the projection on $\nabla\theta_e$ direction of the material change of absolute vorticity due to the work done by pressure gradient force. Although the right hand side of (11) differs in form from that obtained by Bennetts and Hoskins (1979) under the Boussinesq approximation, it is readily shown that they are equivalent.

Assume that an atmospheric parcel at state (P_0, T_0, q) is initially unsaturated, and is later lifted dry-adiabatically to the lifting-condensation-level (LCL) where it becomes saturated at state (P, T, q). Afterwards ($P \leqslant P_c$), the rising parcel keeps the state of saturation. In such a case

$$\theta_e(P_0,\ T_0,\ q) = \theta_e(P,\ T,\ q(T)) = \theta_e(P,\ \alpha), \qquad \text{when} \qquad P \leqslant P_c. \tag{12}$$

This means that when $P \leqslant P_c$, the θ_e surface is parallel to the cross axis between isobaric and isopycnal surface, so that $\alpha(\nabla P \times \nabla \alpha) \cdot \nabla \theta_e \equiv 0$. Therefore, for an atmosphere which is saturated ($p=P_c$, $T=T_d$), or initially unsaturated but later lifted to above LCL, it satisfies

$$\frac{DP_m}{Dt} \equiv 0. \qquad (P \leqslant P_c) \tag{13}$$

or

$$P_m = \alpha \boldsymbol{\zeta}_a \cdot \nabla \theta_e \equiv \text{const.} \qquad (P \leqslant P_c) \tag{14}$$

In other words, for a saturated atmosphere which is adiabatic and frictionless, its MPV is conserved. In such circumstances,

$$\theta_e = \theta(P_c,\ T_c)\exp\left(\frac{Lq}{c_pT_c}\right).$$

From the conservation characteristic of θ, we know that $\theta(P_c,\ T_c) = \theta(P_0,\ T_0)$. We then obtain

$$\theta_e = \theta(P_0,\ T_0)\exp\left(\frac{Lq}{c_pT_c}\right). \tag{15}$$

The calculation of T_c in the above formula is rather tedious. Fortunately the slope of q-isoline in the T-ln$P$ diagram is nearly vertical, so T_c is very close to dewpoint temperature T_d. Then in application, we may replace T_c by T_d, which can be easily calculated from q and P by using the Margules formula.

Similar to the dynamic features of dry atmosphere (Bennetts and Hoskins 1979), the moist atmosphere is moistly and symmetrically stable if $P_m > 0$ and unstable if $P_m < 0$.

IV. MPV AT MOIST ISENTROPES AND VORTICITY DEVELOPMENT

For a saturated, adiabatic and frictionless atmosphere, if the slope of θ_e with respect to isobaric surface is negligible, one can use θ_e as vertical coordinate. The advantage of using such coordinate comes from the fact that along the θ_e surface, $\nabla \theta_e$ vanishes. Therefore, the conservation of MPV takes a simple form:

$$P_m = -g\zeta_\theta \frac{\partial \theta_e}{\partial P} \approx \text{const.}, \tag{16}$$

in which ζ_θ is the vertical projection of $\boldsymbol{\zeta}_a$. By defining convective stability as

$$N_m = \frac{g}{\theta_0}\frac{\partial \theta_e}{\partial z} = -\frac{\rho g^2}{\theta_0}\frac{\partial \theta_e}{\partial P}, \tag{17}$$

Eq. (16) can then be written as

$$\alpha\zeta_\theta N_m \approx \text{const.} \tag{18}$$

Therefore when a parcel moves from a region where convective stability is large to a region where convective stability is small, i. e., from a condensed θ_e region to a loose θ_e region, its cyclonic vorticity will increase. From (16) we can also obtain

$$\frac{1}{\zeta_\theta}\frac{D}{Dt}(\zeta_\theta) = -\frac{1}{\theta_{ep}}\frac{D}{Dt}\theta_{ep}. \tag{19}$$

Then from the definition of θ_e (5) and the following continuity equation in θ-coordinate

$$\frac{\partial}{\partial t}\left(\frac{\partial P}{\partial \theta}\right) + \nabla_\theta \cdot \left(\frac{\partial P}{\partial \theta}\boldsymbol{V}\right) + \frac{\partial}{\partial \theta}\left(\dot{\theta}\frac{\partial P}{\partial \theta}\right) = 0, \tag{20}$$

we can derive the variation equation for convective stability

$$\frac{1}{\theta_{ep}}\frac{D}{Dt}\theta_{ep} = r\left[\nabla_\theta \cdot \boldsymbol{V} + \frac{D}{Dt}\left(\frac{Lq}{c_pT}\right) + \frac{\theta}{\theta_p}\frac{D}{Dt}\frac{\partial}{\partial P}\left(\frac{Lq}{c_pT}\right)\right], \tag{21}$$

where $r = (\theta_p/\theta_{ep})\exp(Lq/c_pT)$, and the variation equation of absolute vorticity per unit mass

$$\frac{D}{Dt}(\zeta_\theta) = -r\zeta_\theta\left[\nabla_\theta \cdot \boldsymbol{V} + \frac{D}{Dt}\left(\frac{Lq}{c_pT}\right) + \frac{\theta}{\theta_p}\frac{D}{Dt}\frac{\partial}{\partial P}\left(\frac{Lq}{c_pT}\right)\right]. \tag{22}$$

The above results show that if $r > 0$, then either wind convergence or latent heat release at θ surface can result in the reduction of convective stability and the increase of cyclonic vorticity.

Figure 1 presents a typical north-south section across a monsoon front A. Cold and dry air from the north and warm and moist air from the south meet at the front in subtropics, and according to Eq. (22), cyclonic vorticity develops. In regions I and II, when air moves southward, the reduction in N_m results in the increase of cyclonic vorticity. To the south of the front there exists a meta convective stable layer $[(\partial \theta_e/\partial P) = 0]$ in the middle troposphere. Under this layer exists a layer which is convectively unstable. When air moves from region IV to region III, θ_{ep} decreases, and according to Eq. (19), cyclonic vorticity increases. Furthermore, once the cold air behind the monsoon front invades the region, convectively unstable energy will be released and result in the development of convection. Finally, let us consider the impacts of near surface sensible heating. From the MPV equation with diabatic heating not neglected

$$\frac{D}{Dt}\left(\alpha\zeta_\theta\frac{\partial \theta_e}{\partial z}\right) = \alpha\zeta_\theta\frac{\partial Q}{\partial z}.$$

Because $Q=0$ above the ground surface, the surface heating then corresponds to $(\partial Q/\partial z)$

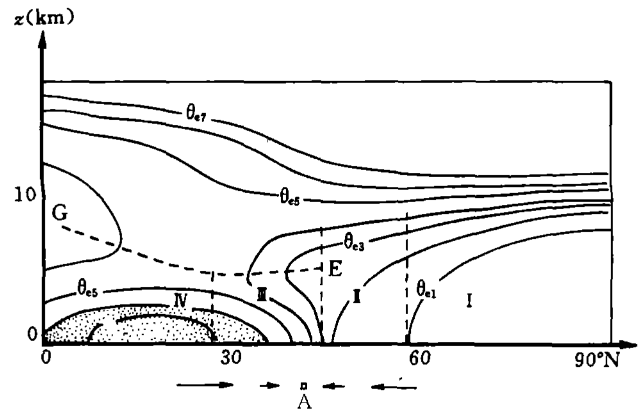

Fig. 1. Distribution of moist isentropic surfaces (fine solid curves) in a typical north-south section across monsoonal front A. Heavy dashed curve indicates the location of neutral convective stability: dotted region is the high θ_e region: and arrows denote the movement of cold and warm air.

<0. Thus for air volume moving over the frontal region, surface heating will reduce its moist potential vorticity in region II, and increase its MPV in region III. As a summary, to the north of the monsoon front the growth or decay of vorticity depends on the effects of convective stability variation in comparison with diabatic heating at the ground. To the south of monsoon front in region III, all elements contribute to the increase of positive vorticity. So it is a region where we expect cyclonic systems to develop. Once rainfall appears, then according to Eq. (22), cyclonic vorticity develops further. Therefore the region around and south of a monsoon front is where heavy precipitation may develop most vigorously.

In June 1991 over East Asia, the subtropical high over the Northwest Pacific was abnormally strong. The trough over the Bay of Bengal was also stronger than normal, and located to the east of its climate mean position. In middle latitudes, there were frequent synoptic scale

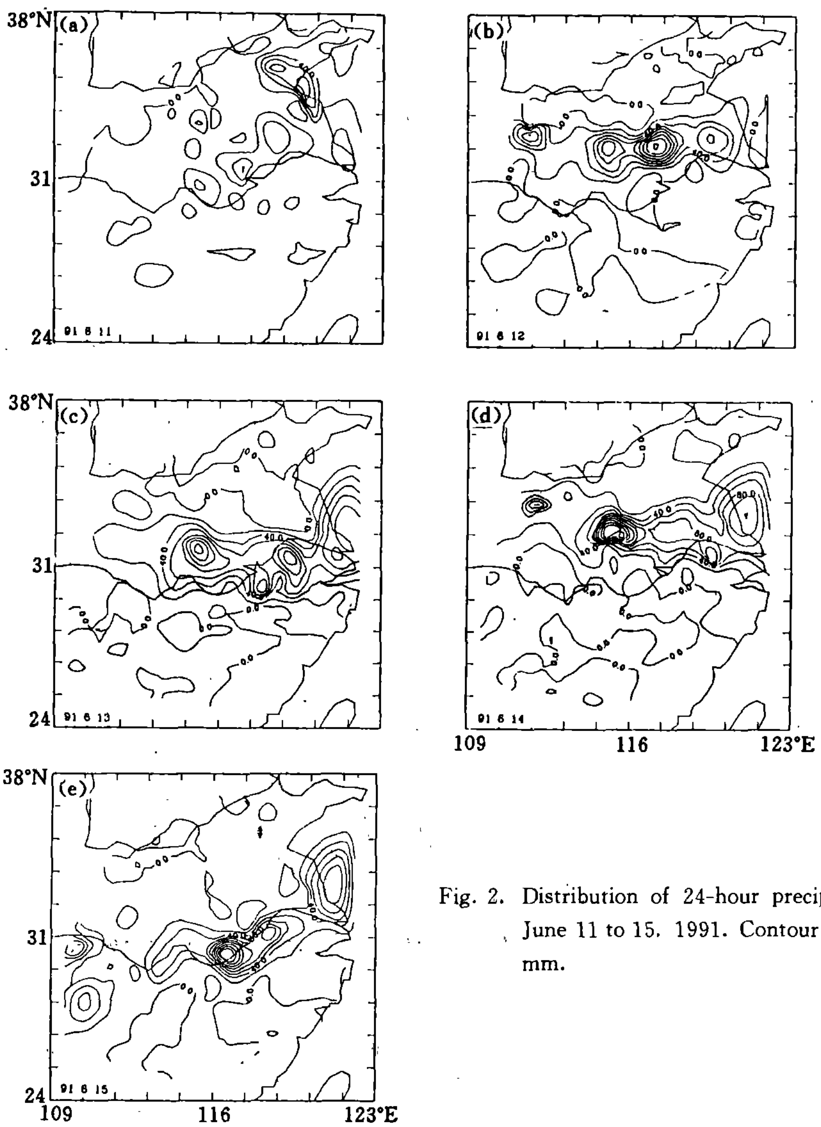

Fig. 2. Distribution of 24-hour precipitation from June 11 to 15, 1991. Contour interval is 20 mm.

systems propagating eastwards. In the middle of the month, cold air came from northwest China, and intercepted low layer southwesterlies from the Bay of Bengal in the middle and lower reaches of the Changjiang and Huaihe Rivers. Persistent torrential rain was observed in the region from June 11 to 15 (Dong 1991). As shown in Fig. 2, the torrential rain fall centers all exceeded or were close to 150 mm per day, and serious flooding occurred. Figure 3 shows the north-south cross-sections of θ_e along 115°E at 0000 Z from June 9 to 16, 1991. This longitude is chosen because it is typical of the places where persistent rainfall occurred. Initially, warm and moist and convective unstable ($\theta_{ez} < 0$) air was located to the south of 31°N. The cold and dry air from high latitudes was characterized by a front with a band of condensed θ_e surfaces. This gradually moved southward from 50°N. On June 11, this θ_e front invaded the moist-convective unstable region in the south, and torrential rain started to occur in the sector of steep and densed θ_e band, i.e., in regions II and III shown in Fig. 1. Afterwards, cold and warm air converged and torrential rain continued. On June 14, another

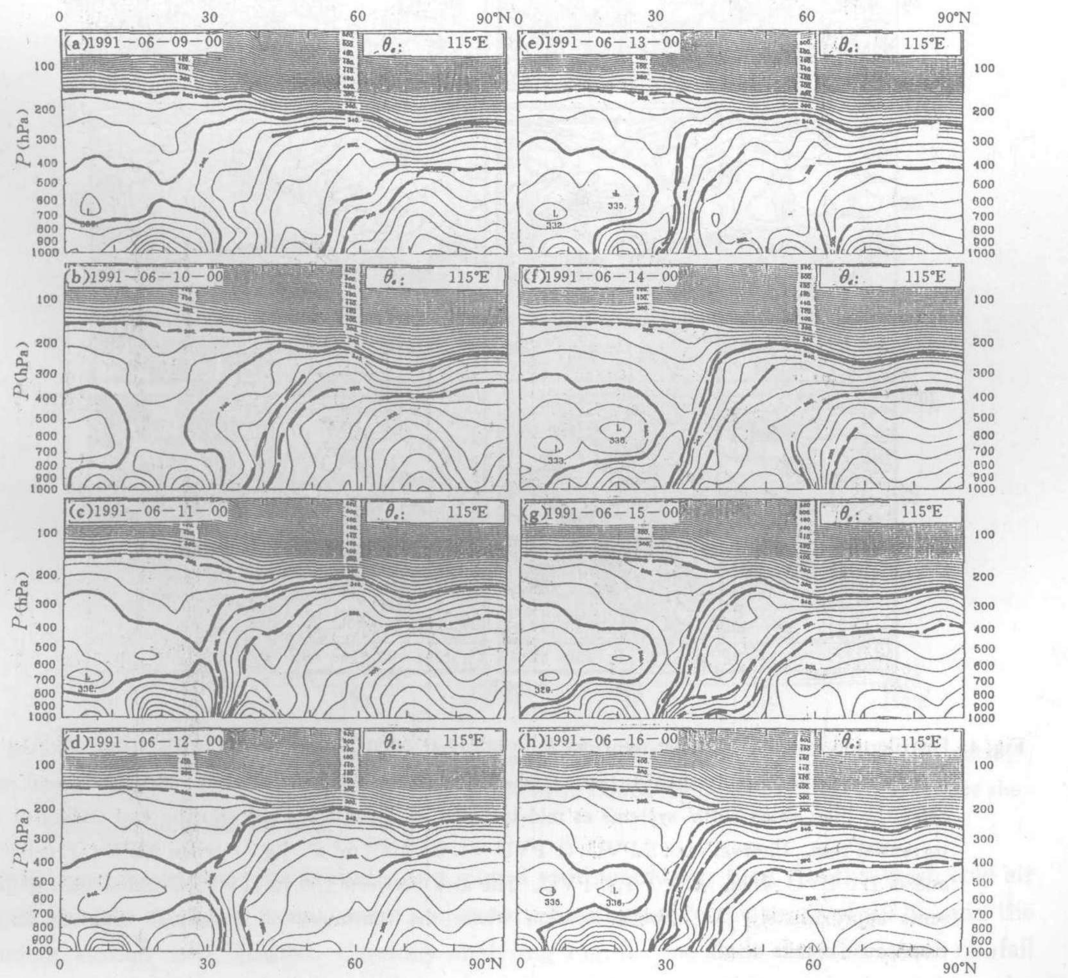

Fig. 3. Distribution of θ_e in the cross-section along 115°E at 0000 Z from June 9 to 16, 1991. Heavy curves indicate the moist isentrope $\theta_e = 345$ K, heavy dashed curves mark the locations of θ_e front and tropopause.

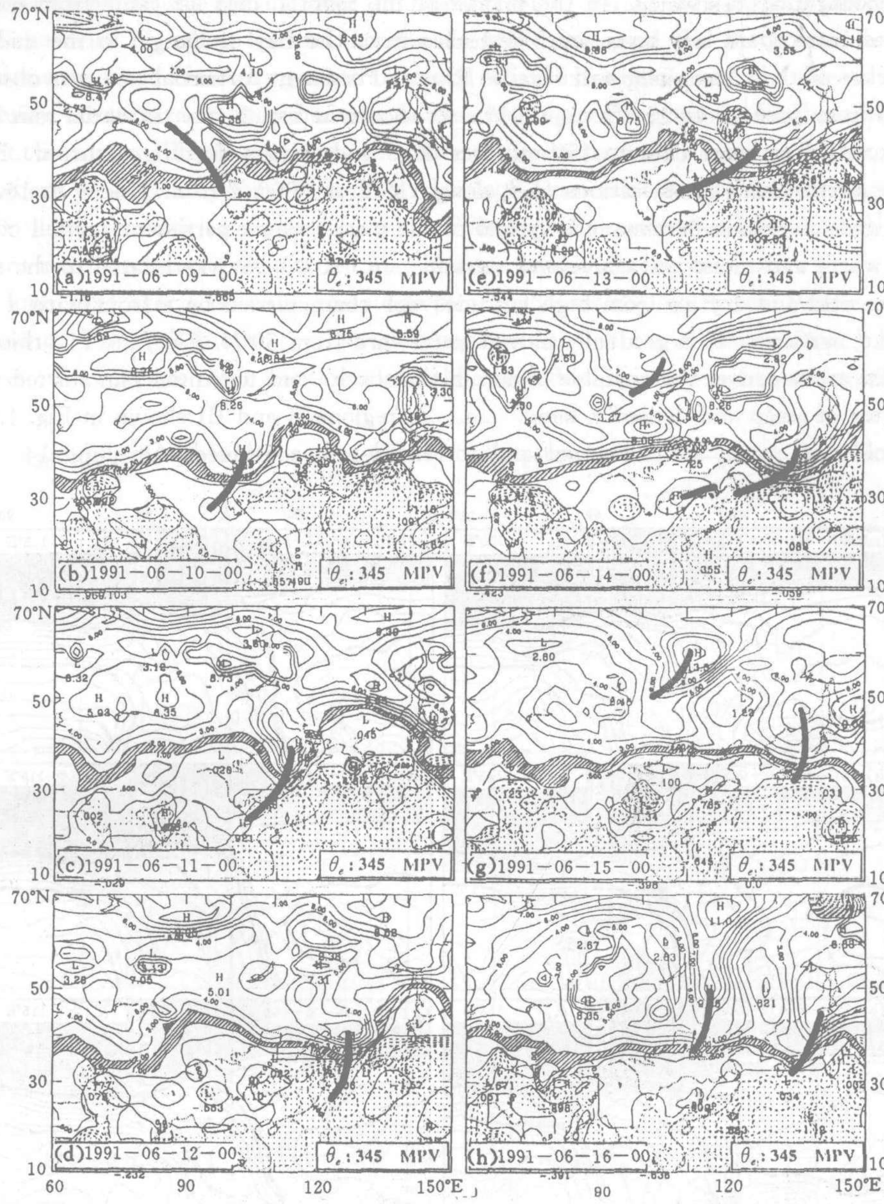

Fig. 4. Distribution of MPV at moist isentrope $\theta_e = 345$ K at 0000 Z from June 9 to 16, 1991. Dotted region denotes the lower branch surface. Dashed curve indicates negative MPV. Heavy segment indicates the high value MPV systems at mid-latitudes which affected the starting and ending of the torrential rain. Interval is 0.5 PVU (1 PVU $= 1.0 \times 10^{-6}$ m^2 s^{-1} kg^{-1}) when MPV $<$ 1.0 PVU, and is 1.0 PVU when MPV $>$ 1.0 PVU. The area between 1.0 to 2.0 PVU is hatched. It presents approximately the latitude location where the continuity of latitudinal variation of the tropopause breaks down.

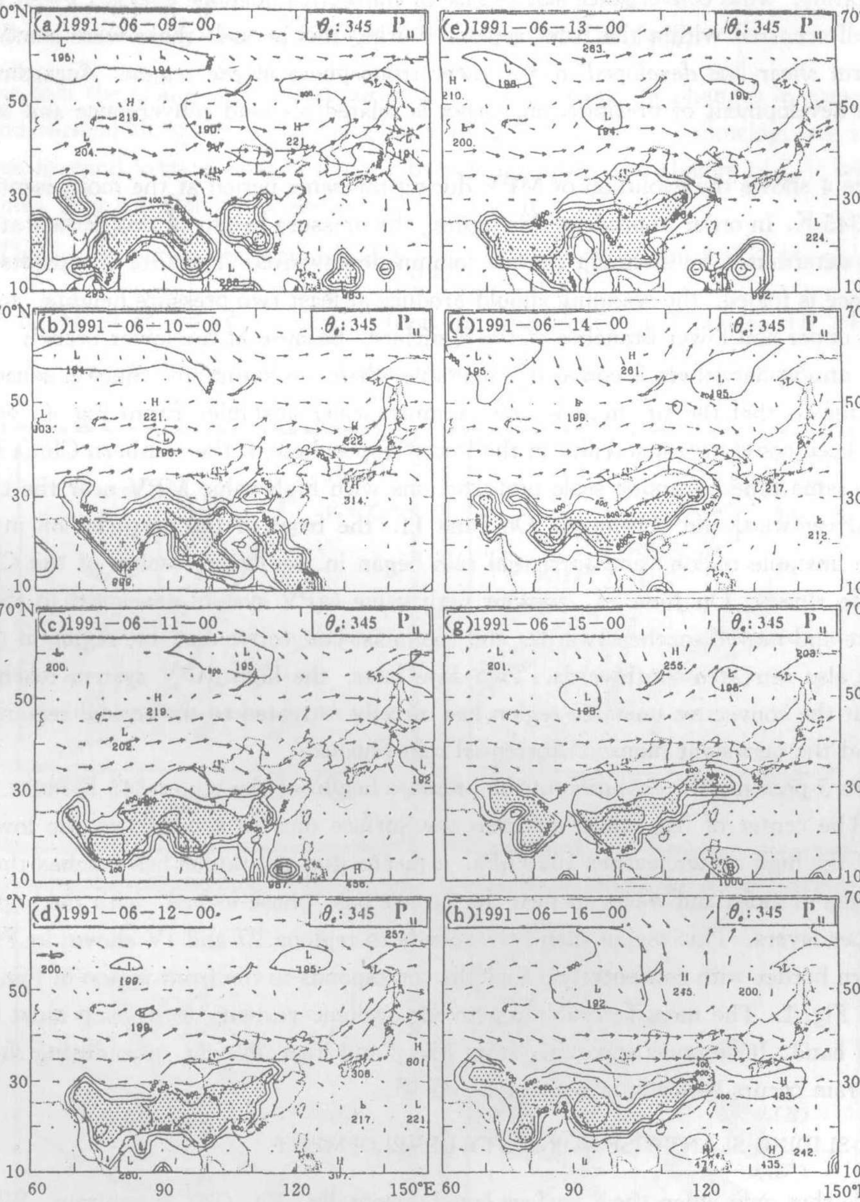

Fig. 5. Evolution of the pressure height of the upper branch of the 345 K moist isentropic surface at 0000 Z from June 9 to 16, 1991. Contour interval is 200 hPa. Dotted region indicates the region where the surface drops below 800 hPa.

subpolar front formed in high latitudes and moved southward. On June 15, this fresh cold air merged into the monsoon front, warm and moist air retreated to the south of 29°N, and the persistent rainfall then finished. Carefully analyzing Fig. 3, one finds that the whole rainfall process can be divided into two stages. On the 11st and 12nd, rainfall occurred mainly to the south of monsoon front, in correspondence with the existence of low layer cold shear line and surface hot wave (Dong 1991). Thus, the occurrence of torrential rain is consistent with the surface heating, wind convergence and release of convective unstable energy. From June 13 to 15, rainfall occurred within the front region. During this period, there were southwesterlies and a warm shear-line developed in the lower troposphere in the region. According to Eq. (22), the development of precipitation vortex is related to wind convergence and latent heat release.

Figure 4 shows the evolution of MPV during the same period at the moist isentropic surface $\theta_e = 345$ K. In order to produce this figure, the pressure height of this surface at each grid point was determined by scanning the air column downwards. Then for gridpoints at which the θ_e surface is folded, the scanning should produce at least two pressure heights, corresponding to the upper and lower branches of the θ_e surface. Because at the lower branch, $(\partial \theta_e/\partial z) < 0$, the atmosphere there is convective unstable when it is saturated. Since ζ_θ is usually positive, this means that the air there is moist-symmetrically unstable. From Fig. 4, we see that there had been convective instability in the lower troposphere in the southern China since June 9. At the same time, synoptic scale perturbations with high value MPV near the tropopause propagated eastward and developed. On June 11, the front of the perturbation invaded the convective unstable region, and torrential rain began in the lower reaches of the Changjiang and Huaihe Rivers. On June 14, another high value MPV system developed to the west of Bagel Lake and moved southeastwards, and the moist-convective unstable region in the southern China also retreated southwards. Two days later, the high MPV system reached North China, but the convective unstable region had already retreated to the coastal region of South China, and the persistent monsoon torrential rain finished.

Figure 5 presents the evolution of the pressure height of the upper-345 K moist isentropic surface. The center of big values indicates the surface dips as a tunnel to the lower troposphere. If the high center reaches 1000 hPa, it means that the tunnel has touched the ground, and the heap of moist and warm air near the surface has "phase-locked" with the high θ_e tunnel in the upper layers. This region then corresponds to regions III and IV shown in Fig. 1; and its northern border with concentrated isopleths corresponds to the front region in Fig. 3 and region II in Fig. 1. The most favorable region for cyclonic vorticity to develop must lie in this condensed band. It becomes apparent, from Fig. 2 and Figs. 5d—5g, that during this period, torrential rain occurs basically in regions II and III.

V. DOWN-SLIDING SLANTWISE VORTICITY DEVELOPMENT

Notice that only when the θ_e surface lays horizontally, Eq. (16) is accurate. When the θ_e surface declines, the accurate form of MPV conservation should be rewritten as

$$\alpha\zeta_\theta |\nabla\theta_e| = \text{const.},$$

where ζ_θ is the projection of $\boldsymbol{\zeta}_a$ on $\nabla\theta_e$. If $\nabla\theta_e$ surfaces are planes, and $\nabla\theta_e$ is constant, the conservation of MPV can be expressed as the head point of the vector α being at a constant θ_e plane (refer to Fig. 6). If z-coordinate is adopted, then

$$P_m = \alpha\zeta_z \frac{\partial \theta_e}{\partial z} + \alpha\zeta_s \frac{\partial \theta_e}{\partial S},$$

where ζ_z and ζ_s are the vertical and horizontal components of $\boldsymbol{\zeta}_a$, respectively, and $|\zeta_s| = \left|\frac{\partial V_m}{\partial z}\right|$, where V_m is the horizontal wind component perpendicular to, and positive on the right side of $\boldsymbol{\zeta}$. Now, the conservation of MPV can be stated as

$$P_m = \alpha\zeta_z \frac{\partial \theta_e}{\partial z} + \alpha\zeta_s \frac{\partial \theta_e}{\partial S} = \alpha\zeta_\theta |\nabla \theta_e| = \text{const}. \tag{23}$$

This means that the change of vertical vorticity can result from the changes in convective stability, wind vertical shear, or moist baroclinity $(\partial \theta_e/\partial S)$. In the following, we study how the changes in wind vertical shear or moist baroclinity affect the change of ζ_a, when the θ_e plane declines. For simplicity, we assume $(\partial/\partial X) \equiv 0$.

(1) The atmosphere is convective stable $\frac{\partial\theta_e}{\partial z} > 0$, and $\nabla \theta_e = \text{const}$. Let the projection on $\nabla \theta_e$ of $\alpha\boldsymbol{\zeta}_a$ be $\overline{AB} = \alpha\zeta_\theta = \alpha\boldsymbol{\zeta}_a \cdot \frac{\nabla \theta_e}{|\nabla \theta_e|}$, then conservation of MPV means $\overline{AB}$ being constant. In other words, in its later movement, the arrow point of the vector $\alpha\boldsymbol{\zeta}_a$ of the parcel

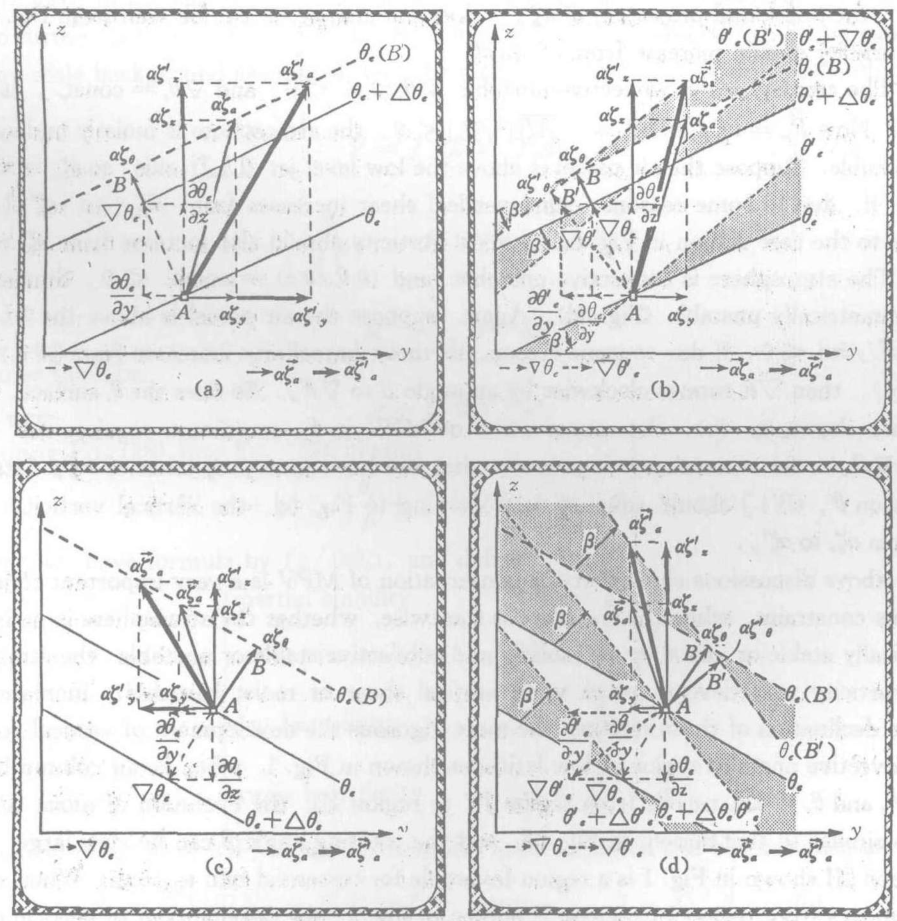

Fig. 6. Under the constraint of conservation of moist potential vorticity, in convective stable (a and b) and unstable (c and d) atmosphere, the increase in vertical shear of horizontal wind (a and c) or in moist baroclinity (b and d) can result in the development of vertical vorticity if and only if the θ_e surfaces are slantwise. Fine solid lines are θ_e lines; fine dashed lines are changed θ_e; and heavy dashed lines are trajectory of the head of absolute vorticity vector per unit mass (see text for details).

should lie on the θ_e plane which passes through point B, i.e., θ_e (B). On the other hand, according to Fig. 6a, Eq. (23) can be rewritten as

$$P_m = \alpha\zeta_z \frac{\partial \theta_e}{\partial z} + \alpha\zeta_y \frac{\partial \theta_e}{\partial y}, \qquad \zeta_y = \frac{\partial U}{\partial z}. \tag{24}$$

Suppose, due to some reasons, the vertical wind shear is increased from $\alpha\zeta_y$ to $\alpha\zeta'_y$. Since the head point of the new vector $\alpha\boldsymbol{\zeta}_a'$ should lie on θ_e (B), the vertical vorticity has to increase from $\alpha\zeta_z$ to $\alpha\boldsymbol{\zeta}_z'$.

(2) The atmosphere is convective stable, and $(\partial \theta_e/\partial z) = \text{const.} > 0$. Suppose, due to some reasons, its moist baroclinity increases from $|(\partial \theta_e/\partial y)|$ to $|(\partial \theta'_e/\partial y)|$, as shown in Fig. 6b. This means that $\nabla\theta_e$ and, of course, θ_e planes rotate counter-clockwise by an angle β. Let the new projection on $\nabla\theta'_e$ of the changed vector $\alpha\boldsymbol{\zeta}_a'$ be $\overline{AB'}$, then conservation of MPV requires 1) $\overline{AB'} = \overline{AB}|\nabla\theta_e|/|\nabla\theta'_e|$, and 2) the arrow point of $\alpha\boldsymbol{\zeta}_a'$ should lie on $\theta'_e(B')$. Since $\alpha\zeta_y$, the horizontal projection of $\alpha\boldsymbol{\zeta}_a'$, does not change, it can be seen from Fig. 6b that vertical vorticity should increase from $\alpha\zeta_z$ to $\alpha\zeta'_z$.

(3) The atmosphere is convective unstable $(\partial \theta_e/\partial z) < 0$; and $\nabla\theta_e = \text{const.}$, as shown in Fig. 6c. Now $P_m = \alpha\boldsymbol{\zeta}_a' \cdot \nabla\theta_e = -\overline{AB}|\nabla\theta_e| < 0$, the atmosphere is moistly and symmetrically unstable. Suppose the air parcel is above the low level jet (LLJ) axis, so $\alpha\zeta_y = \alpha(\partial U/\partial y) < 0$. If, due to some reasons, wind vertical shear increases from $|\alpha\zeta_y|$ to $|\alpha\zeta'_y|$, then analogous to the case shown in Fig. 6a, vertical vorticity should also increase from $\alpha\zeta_z$ to $\alpha\zeta'_z$.

(4) The atmosphere is convective unstable, and $(\partial \theta_e/\partial z) = \text{const.} < 0$. Similarly it is moist-symmetrically unstable (Fig. 6d). Again, suppose the air parcel is above the LLJ, and $\alpha\zeta_y = \alpha|\partial U/\partial z| < 0$. If due to some reason, its moist baroclinity increases from $|\partial \theta_e/\partial y|$ to $|\partial \theta'_e/\partial y|$, then $\nabla\theta_e$ rotates clockwise by an angle β to $\nabla\theta'_e$. So does the θ_e surface. Similar to the case shown in (b), the conservation of MPV in θ_e-coordinate requires $\overline{AB'} = \overline{AB}|\nabla\theta_e|/|\nabla\theta'_e|$. In z-coordinate it presents that the horizontal projection of $\alpha\boldsymbol{\zeta}_a'$ [its arrow point lies on θ'_e (B')] should equal $\alpha\zeta_y$. According to Fig. 6d, the vertical vorticity will increase from $\alpha\zeta_z$ to $\alpha\zeta'_z$.

The above discussions show that the conservation of MPV is a very important constraint. Under this constraint, when the θ_e surface is slantwise, whether the atmosphere is moistly and symmetrically stable or unstable, or moistly and convective stable or unstable, the atmospheric vertical vorticity may develop when wind vertical shear or moist baroclinity increases. The larger the declination of the θ_e surface, the more vigorous the development of vertical vorticity. In the convective unstable region at low latitudes shown in Fig. 1, when an air column bounded between θ_e and $\theta_e + \Delta\theta_e$ travels from region IV to region III, the evolution of moist isentropic surface is similar to that shown in Fig. 6d, and the rotating angle β can be very large. Therefore, region III shown in Fig. 1 is a region favorable for torrential rain to occur. When mid-latitude air moves from region I to region II shown in Fig. 1, the development of vertical cyclonic vorticity can be explained by Fig. 6b.

VI. ISOBARIC MOIST POTENTIAL VORTICITY AND SLANTWISE VORTICITY DEVELOPMENT

By introducing the hydrostatic approximation to (13) and (14), adopting p-coordinate, and assuming the horizontal variation of vertical velocity is much smaller than the vertical shear of horizontal wind and can be neglected, the expression of MPV then becomes

$$P_m = - g(f\boldsymbol{k} + \nabla_p \times \boldsymbol{V}) \cdot \nabla_p \theta_e = \text{const.} \tag{25}$$

Define the vertical component of MPV as the first component, and the horizontal component the second component, i. e.,

$$\begin{cases} MPV1 = - g\zeta_P \dfrac{\partial \theta_e}{\partial p}, \\ MPV2 = - g\boldsymbol{k} \times \dfrac{\partial \boldsymbol{V}}{\partial p} \cdot \nabla_p \theta_e, \end{cases} \tag{26}$$

where $\zeta_p = f + \left(\dfrac{\partial v}{\partial x} - \dfrac{\partial u}{\partial y}\right)_p$, the conservation of MPV in p-coordinate can be expressed as

$$P_m = MPV1 + MPV2 = \alpha\zeta_\theta |\nabla \theta_e| = \text{const.} \tag{27}$$

Since synoptic scale motion closely satisfies the hydrostatic approximation, Eq. (27) is then basically equivalent to Eq. (23) in z-coordinate. Then the theory of slantwise vorticity development proposed in the last section (see Fig. 6) is applicable in the p-coordinate system.

To further understand the physical meaning of Eqs. (26) and (27), let us suppose that the large-scale background associated with the monsoon front satisfies the geostrophic relationship, i. e.

$$\boldsymbol{V} = f^{-1}\boldsymbol{k} \times \nabla_p \Phi,$$

so

$$\frac{\partial \boldsymbol{V}}{\partial P} = - f^{-1}R^* \boldsymbol{k} \times \nabla_P \theta, \tag{28}$$

where

$$R^* = c_p^{-1}P^{-1}R\pi, \tag{29}$$

and Exner function

$$\pi = c_p (PP_0^{-1})^\kappa. \tag{30}$$

Substituting Eq. (28) into Eq. (25) obtains

$$P_m = - g\left(\zeta_p \frac{\partial \theta_e}{\partial p} + f^{-1}R^* \nabla_p \theta \cdot \nabla_p \theta_e\right) = \text{const.} \tag{31}$$

Multiply the above formula by $fg/(\alpha\theta_0)$, and define

$$\begin{cases} \text{inertial stability} & F^2 = f\zeta_p, \\ \text{convective stability} & N_m^2 = \dfrac{g}{\theta_0}\dfrac{\partial \theta_e}{\partial z}, \\ \text{dry baroclinity} & S^2 = \dfrac{g}{\theta_0}|\nabla_p \theta|, \\ \text{moist baroclinity} & S_m^2 = \dfrac{g}{\theta_0}|\nabla_p \theta_e|, \end{cases} \tag{32}$$

then the conservation of MPV under geostrophic approximation can be expressed as

$$P_m = \frac{\alpha\theta_0}{fg}(F^2N_m^2 - S^2S_m^2\cos\gamma) = \text{const.}, \qquad \gamma = (\nabla_p \theta, \nabla_p \theta_e). \tag{33}$$

From this formula and Eq. (25) the material change of absolute vorticity under the geostrophic constraint becomes

$$\frac{\mathrm{D}}{\mathrm{D}t}\zeta_p = - \zeta_p \frac{\mathrm{D}}{\mathrm{D}t}\ln\left(\frac{\partial \theta_e}{\partial p}\right) - \left(fg^2 \frac{\partial \theta_e}{\partial p}\right)^{-1} \frac{\mathrm{D}}{\mathrm{D}t}(\alpha\theta_0 S^2 S_m^2 \cos\gamma). \tag{34}$$

Usually $|\alpha| < (\pi/2)$; especially when the atmosphere is saturated, $\alpha = 0$. Then from Eqs. (33) and (34) we obtain the following conclusions.

(1) Under the constraint of geostrophic approximation, the horizontal component of MPV is negative, i.e., in Eq. (27) $MPV2<0$;

(2) For a moist-symmetrically stable atmosphere, if initially the atmosphere is inertially and convective stable ($F^2>0$, $N_m^2>0$), then in its later movement, it will still be inertially and convective stable. In other words, under the constraint of geostrophic approximation, an initially stable system cannot become unstable by only advection;

(3) When dry and moist baroclinities keep constant, the decrease of the magnitude of convective stability will result in an increase of absolute vorticity;

(4) In moistly and symmetrically stable atmosphere, when convective stability keeps constant, the increase in dry or moist baroclinity will result in the increase of absolute vorticity (refer to Figs. 6a and 6b);

(5) In a moistly and symmetrically unstable atmosphere, when convective stability keeps constant, then the increase in dry and moist baroclinities will result in the decrease of absolute vorticity. Since in geostrophic case, $\alpha\zeta_y$ and $\partial\theta_e/\partial y$ in Figs. 6c and 6d should possess opposite signs. This conclusion is then evident.

Monsoon torrential rain in the real atmosphere usually occurs in convective unstable situation, with dry and moist baroclinities and vertical vorticity increasing together, and with positive $MPV2$ appearing in the lower troposphere. They are all in contrast to the above conclusions obtained using the geostrophic approximation. It is therefore inadequate to use the geostrophic approximation for such a diagnosis of torrential rain associated with monsoon frontogenesis in a convective unstable atmosphere.

VII. MPV ANALYSIS AT ISOBARIC SURFACES

In this section we will analyze the evolution of moist potential vorticity at isobaric surfaces during the process of persistent torrential rain occurring in the period of June 11—15, 1991. By doing so, we examine the applicability of MPV in the diagnosis of monsoon torrential rain. Figure 7 shows the evolution of $MPV1$ at 200 hPa. The area between 2.0 and 3.0 PVU is hatched so that the perturbation near the edge of troposphere can be traced much easier. It can be seen that the high $MPV1$ perturbation over Northwest China on June 9 moved eastward and developed later. On June 11, this perturbation crossed the middle reaches of Huanghe and Changjiang Rivers, and torrential rain in the Changjiang and Huaihe River reaches began to appear. On the 14th, a new high $MPV1$ system developed over Siberia and started to move southeastward. On the 16th, it already passed North China and moved eastward, and the torrential rain finished. Comparing Fig. 7 with Fig. 4, one finds that in middle and high latitude regions, they are very similar. The evolution of the perturbations near tropopause is similar too. This is because in middle and high latitudes, the location of moist isentrope $\theta_e=345$ K is very close to 200 hPa (Fig. 3). In addition, at 200 hPa, $MPV2\ll MPV1$, so P_m and $MPV1$ are comparable. At middle and low latitudes, the θ_e surface declines gradually, the ζ_θ component which is extrapolated from the observed (u, v) fields is not perpendicular to the θ_e surface. In these regions, the MPV distribution shown in Fig. 4, therefore, possesses considerable errors.

Figure 8 shows the evolution of $MPV1$ at 700 hPa in the same period. It can be identified that its distribution in the lower troposphere is in good correspondence with that in upper layers. For example, a high $MPV1$ system which was in Northwest China on June 9 traveled regularly southeastwards. Since June 11, the high $MPV1$ air over North China which was convective stable confronted along the Changjiang-Huaihe River reaches with the convective unstable atmosphere over South China. Persistent torrential rain then started to occur near the

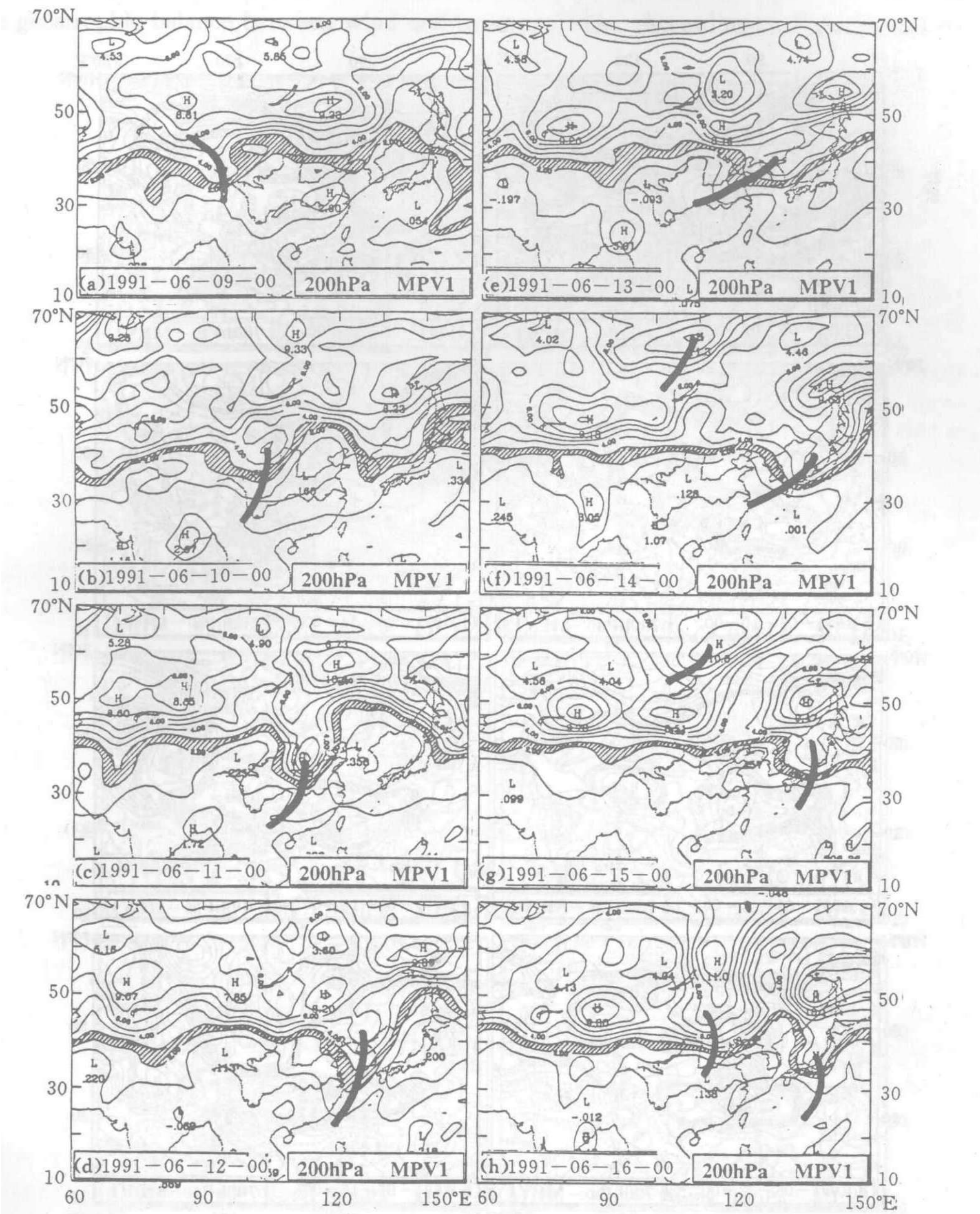

Fig. 7. Evolution of the vertical component $MPV1$ of moist potential vorticity at 200 hPa at 0000 Z from June 9 to 16, 1991. Heavy segment indicates the high value MPV system which affects the location of torrential rain. Contour interval is 1.0 PVU. The area between 2.0 and 3.0 PVU is hatched.

edge of the convective unstable region in front of the high value $MPV1$ system. On the 16th, as the convective stable air occupied the region south to the Changjiang River, torrential rain stopped.

Shown in Fig. 9 is the evolution of horizontal component $MPV2$ at 700 hPa in the same period. It is remarkable that during this period along the Changjiang River, there existed an

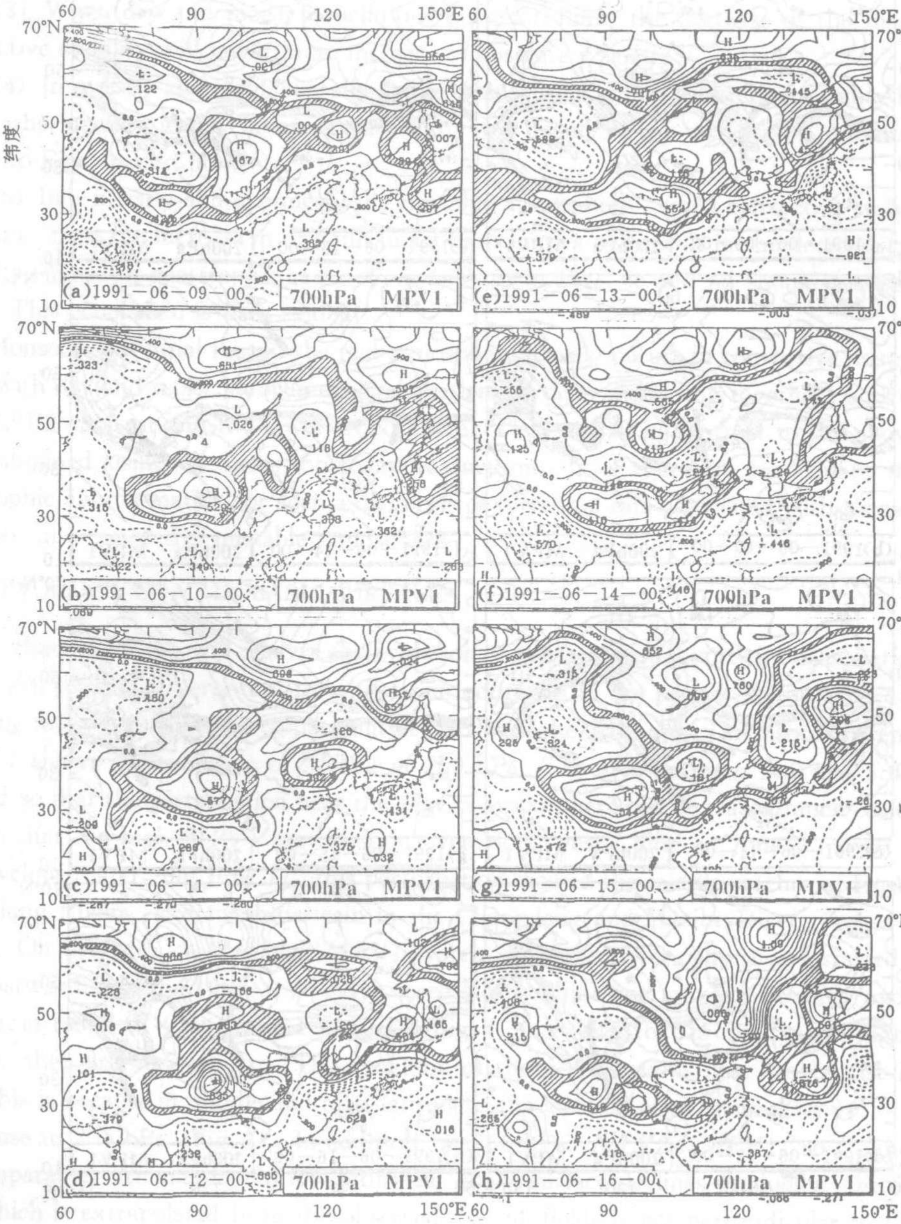

Fig. 8. Evolution of the vertical component $MPV1$ of moist potential vorticity at 700 hPa at 0000 Z from June 9 to 16, 1991. Dashed curves denote negative value. Contour interval is 0.1 PVU. The area between 0.1 and 0.2 PVU is hatched.

elongated band of positive $MPV2$. This is because in the period at 700 hPa, the warm and moist air was in the south to the Changjiang River, and the LLJ existed below 700 hPa (Dong 1991). Thus along the Changjiang River, $(\partial U/\partial z)<0$, $(\partial \theta_e/\partial y)<0$, and $MPV2$ there became positive. The appearance of positive $MPV2$ in the Changjiang-Huaihe Rivers region during the period of monsoon torrential rain thus revealed that in the area, there did not exist the geostrophic balance between wind and pressure fields. According to Figs. 6c and 6d, the

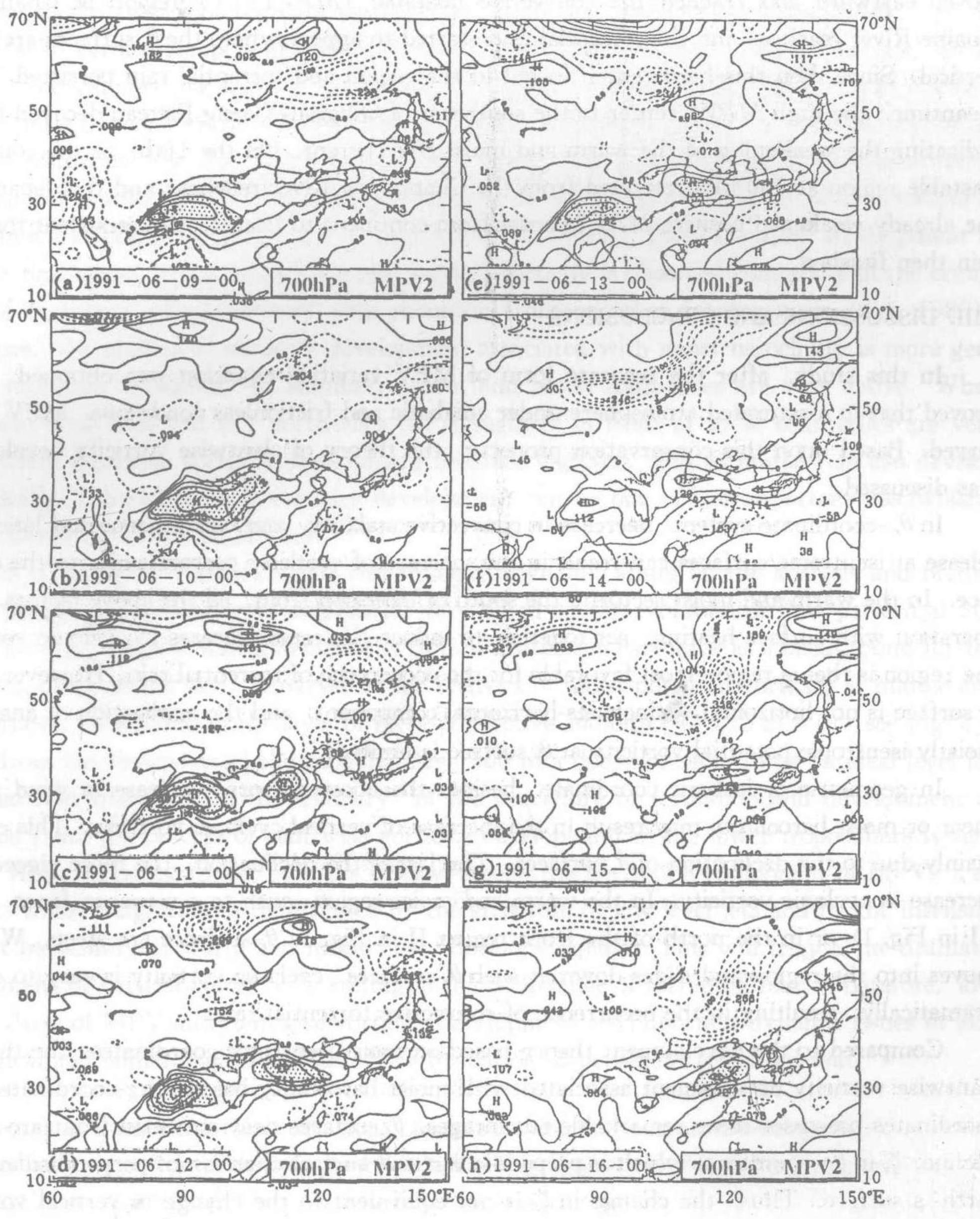

Fig. 9. Evolution of the horizontal component $MPV2$ of moist potential vorticity at 700 hPa at 0000Z from June 9 to 16, 1991. Dashed curves denote negative value. Contour interval is 0.05 PVU. Dotted area presents high positive region with $MPV2>0.1$ PVU.

increase in the intensity of LLJ or of warm and moist air advection will increase $MPV2$ and ζ_z, in favor of the strengthening of precipitation. Therefore the movement of positive $MPV2$ in the lower troposphere can serve as a tracer of the activities of LLJ and warm and moist current. As seen in Fig. 9. a high positive $MPV2$ center was located in the southeast flank of Qinghai-Xizang Plateau on June 9. Later on, it stretched eastward along the Changjiang River. On the 11th, a new positive $MPV2$ center which was separated from the main center moved eastward and reached the convective unstable ($MPV1 < 0$) region in Changjiang-Huaihe River reaches, and the torrential rain started to appear where the θ_e surfaces are almost vertical. Since then this high center stayed in the region and torrential rain persisted. In the meantime, the high $MPV2$ center to the southeast of Qinghai-Xizang Plateau decayed locally, indicating the weakening of the warm and moist SW current. On the 16th, as the convective unstable region at 700 hPa retreated from the Changjiang River reaches, and the departure of the already weakened positive $MPV2$ center from continent to Pacific, the persistent torrential rain then finished.

VIII. DISCUSSIONS AND CONCLUSIONS

In this study, after the accurate form of MPV variation equation was obtained, it was proved that in a saturated atmosphere under adiabatic and frictionless conditions, MPV is conserved. Based upon this conservation property, the theory of slantwise vorticity development was discussed.

In θ_e -coordinate system, decrease in convective stability, and convergence and latent heat release at isentropic surfaces can result in the increase of vorticity perpendicular to the θ_e -surface. In the warm and moist sector to the south of monsoon front, all the above factors, in co-operation with surface heating, act together to induce the rapid increase in cyclonic vorticity, the region is then a region most favorable for the occurrence of torrential rain. However, when θ_e surface is not horizontal, ζ_θ includes horizontal component, and the application of analysis of moistly isentropic potential vorticity at θ_e surface is limited.

In geometric or isobaric coordinate, besides the above factors, increase in wind vertical shear or moist baroclinity may result in the increase of vertical cyclonic vorticity. This effect is mainly due to the declination of θ_e surfaces. The larger the declination, the more vigorous the increase in cyclonic vorticity. In the warm and moist region south to a monsoon front (region III in Fig. 1) or in the north of the front region II in Fig. 1, θ_e surfaces are steep. When air moves into the region and slides down at such θ_e surfaces, cyclonic vorticity is easy to develop dramatically, resulting in the occurrence of convective torrential rain.

Compared to the development theory based on moist isentropic coordinates, the theory of slantwise vorticity development associated with moist baroclinity based on z-coordinates or p-coordinates possesses some remarkable advantages. θ_e surfaces near monsoon front are usually decline. ζ_θ in θ_e -coordinate which is perpendicular to θ_e surface then is not perpendicular to the earth's surface. Thus, the change in ζ_θ is not equivalent to the change in vertical vorticity. When z-coordinate or p-coordinate is used, the summation of the horizontal and vertical component of P_m is conserved. Now the change in ζ_z (ζ_p) is determined either by the changes in convective stability, wind vertical shear or by moist baroclinity. Therefore, increase in wind vertical shear or by moist baroclinity can result in the development of vertical cyclonic vorticity. If geostrophic approximation is assumed, the conservation of MPV can be stated as follows: for unit mass column, the difference between the product of inertia stability and convective stabilities and the product of dry and moist baroclinities is constant. However, the results from this study show that geostrophic approximation is inadequate for the analysis of torrential rain of convective unstable type associated with monsoon front.

Finally, it is worthwhile to note that the theory of slantwise vorticity development is not the same as the theory of vorticity development associated with vorticity conversion from its horizontal to vertical component due to the uneven lifting of a vortex. In the latter case, an increase in vertical vorticity requires a decrease in horizontal vorticity. The theory developed here is based upon the conservation characteristics of moist potential vorticity. It requires declination of moist isentropic surfaces. According to this theory, the development of vertical vorticity may be accompanied by the concurrent development of horizontal vorticity or moist baroclinity, and is much stronger than that due to uneven vortex lifting. The concurrent development of wind vertical shear, moist baroclinity and vertical vorticity is observed commonly in the occurrence of torrential rain associated with monsoon front or other frontogenesis (Tao 1980). Therefore, the process of vorticity development associated with moist baroclinity is more general in monsoon dynamics. In summer, warm and moist southerlies are very active. When they meet with cold and dry northerlies the θ_e surfaces in front of these southerlies are very steep, there slantwise vorticity development becomes vigorous, and torrential rain can develop dramatically. Therefore such vorticity development can be one of the important mechanisms for the formation of torrential rain.

Due to historical reasons, some climatological dynamic study on the analysis and prediction of persistent torrential rain emphasizes very much on the evolution of flow pattern at 500 hPa. There is no doubt that kinematically 500 hPa situation can serve as a background for the prediction of torrential rain. However in the analysis of moist potential vorticity at middle and low latitudes, 500 hPa is in the layer of meta-convective stability [$(\partial \theta_e/\partial z)=0$), see Fig. 2]. Thus, from the viewpoint of thermodynamics, 500 hPa does not seem to be an ideal level for torrential rain analysis. On the contrary, in the procedure of formation and development of torrential rain, the process of slantwise vorticity development in the lower troposphere is very active. When moist isentropic surfaces become steep, the horizontal component of MPV, i. e. *MPV*2, whose magnitude is determined by the structure of low level jets and by the intensity of moist baroclinity of warm and moist flow, develops rapidly. This will trigger the dramatic development of vertical vorticity, resulting in the occurrence of torrential rain. Therefore, low level analysis of MPV and slantwise vorticity development are important dynamic issues in meteorological and climatological studies of the formation of persistent torrential rain.

The authors would like to thank Mr. Dong Liqing of the Chinese National Meteorological Center for providing the basic material for this study, and thank Ms. Sun Yanbin and Ms. Wang Xuan for typing the draft.

REFERENCES

Bennetts, D. A. and Hoskins, B. J. (1979). Conditional symmetric instability—a possible explanation for frontal rainbands. *Quart. J. Roy. Meteor. Soc.*, **105**: 945—962.

Dong Liqing (1991). Persistent torrential rain in Changjiang-Huaihe River reaches, and abnormal temperature in most part of China. *Meteor. Monthly*, **17** (9): 58—61 (in Chinese).

Ertel, H. (1942). Ein neuer hydrodynamischer Wirbdsatz. *Meteorology*, Zeitschr, Braunschweig, 277—281.

Hoskins, B. J., McIntyre, M. E. and Robertson, A. W. (1985). On the use and significance of isentropic potential vorticity maps. *Quart. J. Roy. Meteor. Soc.*, **111**: 877—946.

Tao Shiyan (1980). *Torrential Rain in China*. Science Press, 225pp. (in Chinese).